

ORIGINAL RESEARCH COMMUNICATION

# Selenoprotein M Promotes Hypothalamic Leptin Signaling and Thioredoxin Antioxidant Activity

Ting Gong,<sup>1</sup> Ann C. Hashimoto,<sup>2</sup> Alexandru R. Sasuclark,<sup>2</sup> Vedbar S. Khadka,<sup>3</sup>  
Alexandra Gurary,<sup>4</sup> and Matthew W. Pitts<sup>2</sup>

## Abstract

**Aims:** Selenoproteins are an essential class of proteins involved in redox signaling and energy metabolism. However, the functions of many selenoproteins are not clearly established. Selenoprotein M (SELENOM), an endoplasmic reticulum (ER)-resident oxidoreductase bearing structural similarity to thioredoxin (TXN), is among those yet to be fully characterized. This protein is highly expressed in hypothalamic regions involved in leptin signaling and has been previously linked to energy metabolism. Herein, we performed a series of studies using *in vivo* and *in vitro* models to probe the specific influence of SELENOM on hypothalamic leptin signaling and assess SELENOM-regulated pathways.

**Innovation and Results:** Our initial experiment *in vivo* demonstrated that (i) leptin promotes hypothalamic expression of SELENOM and (ii) leptin-induced STAT3 phosphorylation is impeded by SELENOM deficiency. Additional *in vitro* studies using mHypoE-44 immortalized hypothalamic neurons corroborated these findings, as SELENOM deficiency obstructed downstream STAT3 phosphorylation and cytosolic calcium responses evoked by leptin treatment. Correspondingly, SELENOM overexpression enhanced leptin sensitivity. Microarray analysis conducted in parallel on hypothalamic tissue and mHypoE-44 cells revealed multiple genes significantly affected by SELENOM deficiency, including thioredoxin interacting protein, a negative regulator of the TXN system. Further analysis determined that (i) SELENOM itself possesses intrinsic TXN activity and (ii) SELENOM deficiency leads to a reduction in overall TXN activity. Finally, mHypoE-44 cells lacking SELENOM displayed diminished activation of the nuclear factor kappa-light-chain enhancer of activated B-cells (NF- $\kappa$ B) signaling pathway and increased susceptibility to ER stress-mediated cell death.

**Conclusion:** In sum, these findings establish SELENOM as a positive regulator of leptin signaling and TXN antioxidant activity in the hypothalamus. *Antioxid. Redox Signal.* 35, 775–787.

**Keywords:** endoplasmic reticulum, hypothalamus, leptin, selenoprotein, thioredoxin

## Introduction

SELENOPTOTEINS ARE AN essential class of proteins involved in redox signaling that have been increasingly implicated in energy metabolism. These proteins are characterized by the co-translational incorporation of selenium (Se) in the form of selenocysteine (Sec) and include the glutathione peroxidases, thioredoxin reductases (TXNRDs), iodothyronine deiodinases, and a host of additional Sec-

containing proteins with undetermined molecular functions. Among the latter category is SELENOM (selenoprotein M), an uncharacterized endoplasmic reticulum (ER)-resident oxidoreductase that has been previously linked to  $\text{Ca}^{2+}$  homeostasis and energy metabolism. Structurally, SELENOM bears similarity to thioredoxin (TXN), as it contains a TXN-fold in its tertiary structure and a CxxU (U = Sec) active site that is believed to mediate disulfide exchange (9). SELENOM is also abundantly expressed in the brain, particularly

<sup>1</sup>Department of Molecular Biosciences and Bioengineering, University of Hawaii, Honolulu, Hawaii, USA.

Departments of <sup>2</sup>Cell and Molecular Biology, and <sup>4</sup>Tropical Medicine, Medical Microbiology, and Pharmacology, John A. Burns School of Medicine, University of Hawaii, Honolulu, Hawaii, USA.

<sup>3</sup>Bioinformatics Core in the Department of Complementary and Integrative Medicine, John A. Burns School of Medicine, University of Hawaii, Honolulu, Hawaii, USA.

### Innovation

Although selenium (Se) has been increasingly implicated in energy homeostasis, its influence remains enigmatic, largely because many selenoproteins remain uncharacterized. Selenoprotein M (SELENOM), an ER-resident oxidoreductase, is among those lacking an established molecular function. Herein, by a series of *in vivo* and *in vitro* studies, we identify SELENOM as a positive regulator of leptin signaling and thioredoxin (TXN) activity in the hypothalamus. This work establishes SELENOM as an important player in redox-mediated regulation of leptin signaling and has significant clinical implications for the development of novel therapeutics targeting leptin resistance in metabolic disease.

in hypothalamic regions involved in leptin signaling (32). Our initial characterization of *Selenom*<sup>-/-</sup> global knockout mice led to the unexpected finding that SELENOM exerts a significant influence on energy homeostasis, as *Selenom*<sup>-/-</sup> mice developed increased body weight, elevated white adipose tissue levels, and reduced hypothalamic leptin sensitivity (32). Although leptin resistance eventually became apparent in *Selenom*<sup>-/-</sup> mice, it was not established whether this represented the root cause of the obese phenotype or simply a secondary complication.

Leptin resistance is a hallmark feature of obesity that occurs when increasing leptin levels fail to stimulate energy metabolism and inhibit feeding behavior. One established cause of leptin resistance is chronic ER stress, a phenomenon resulting from the accumulation of misfolded proteins and/or Ca<sup>2+</sup> depletion within this organelle (30, 45). ER stress activates the unfolded protein response, an evolutionarily conserved mechanism to restore cellular homeostasis that is mediated by three parallel signaling pathways, each initiated by a distinct ER-resident transmembrane sensor (15, 37). One of these pathways triggers cytosolic splicing of X-box binding protein 1 (XBP1s) mRNA (20), leading to its translocation to the nucleus where it acts as a transcription factor to upregulate various genes involved in protein folding, including SELENOM (36). Interestingly, evidence also indicates that XBP1s promotes leptin sensitivity, as enforced

expression of XBP1s enhances leptin signaling *in vitro*, whereas neuronal-specific XBP1s ablation increases susceptibility to diet-induced obesity in mice (30). Based on the aforementioned results and our prior finding that *Selenom*<sup>-/-</sup> mice develop leptin resistance, we hypothesized that SELENOM may be a positive regulator of leptin signaling.

To further investigate this potential role for SELENOM, we conducted a series of studies using *in vivo* and *in vitro* model systems to probe the influence of SELENOM on leptin signaling. In addition, we also performed microarray analysis on both mouse hypothalamic tissue and immortalized hypothalamic cells to identify genes and pathways most affected by SELENOM deficiency. Our results indicate that SELENOM promotes leptin signaling and TXN-antioxidant activity in the hypothalamus.

### Results

We previously reported that on reaching 18–20 weeks of age, *Selenom*<sup>-/-</sup> mice exhibit symptoms of obesity and hypothalamic leptin resistance (32). To determine whether hypothalamic leptin resistance precedes the development of the obese phenotype in *Selenom*<sup>-/-</sup> mice, we performed a leptin challenge on 10-week-old male mice of equal body weight [wild type (WT) = 24.5 ± 0.4 g; *Selenom*<sup>-/-</sup> = 24.1 ± 0.4 g; *n* = 6–7 per genotype] and we assessed downstream Stat3 signaling. Western blot analysis of hypothalamic tissue showed that leptin-induced Stat3 phosphorylation was significantly attenuated in *Selenom*<sup>-/-</sup> mice relative to controls (Fig. 1A, B). Moreover, in control samples, we found that both SELENOM mRNA and protein levels were increased by leptin treatment (Fig. 1C, D), corroborating results from a prior microarray study showing SELENOM upregulation in response to leptin (39).

To further probe the influence of SELENOM on leptin signaling, we performed a series of studies in mHypoE-44 cells, an immortalized cell line derived from embryonic mouse hypothalamic neurons that expresses agouti-related peptide (AGRP) and neuropeptide Y (10). In our initial study, we stably transfected these cells with a SELENOM-targeted short hairpin RNA (shRNA) construct under the control of the Tet-On<sup>®</sup> inducible system. Doxycycline-mediated induction of this construct was observed to knock down

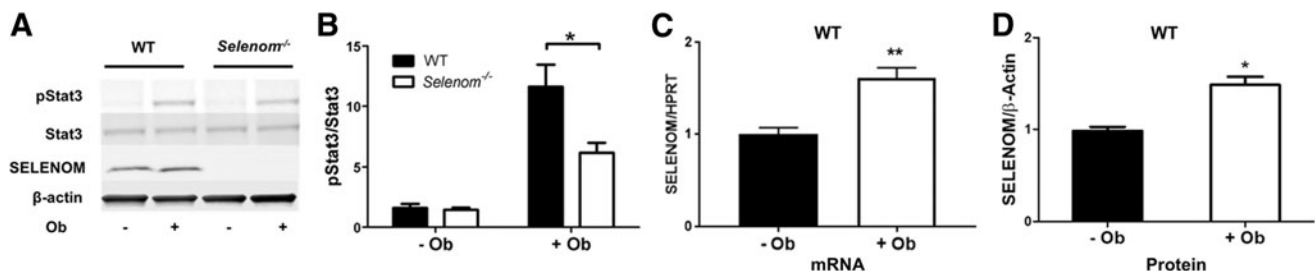


**FIG. 1. SELENOM promotes hypothalamic leptin signaling *in vivo*.** (A) Western blot analysis of leptin-induced signaling in hypothalamic tissue derived from 10-week-old male wild-type and *Selenom*<sup>-/-</sup> mice of comparable body weight. Animals were fasted overnight, challenged with an intraperitoneal injection of leptin (Ob) (1 μg leptin/gram body weight), and sacrificed 60 min later (*n* = 3–4 per group). (B) Two-way ANOVA analysis revealed main effects for leptin ( $F_{(1,8)} = 53.35$ ,  $p < 0.001$ ), genotype ( $F_{(1,8)} = 7.68$ ,  $p = 0.0242$ ), and a significant interaction ( $F_{(1,8)} = 6.81$ ,  $p = 0.0311$ ). Post-tests showed that leptin-induced Stat3 phosphorylation was diminished in *Selenom*<sup>-/-</sup> samples ( $t_4 = 3.806$ ,  $p < 0.05$ ). (C) Leptin treatment elevated SELENOM mRNA levels in WT samples ( $t_8 = 4.628$ ,  $p = 0.0017$ ). (D) Leptin treatment increased SELENOM protein levels in WT samples ( $t_4 = 3.364$ ,  $p = 0.0282$ ). \* $p < 0.05$ , \*\* $p < 0.01$  compared with control group. ANOVA, analysis of variance; SELENOM, selenoprotein M; WT, wild type.

SELENOM protein levels to ~25% of control levels (Fig. 2A). In accord with our *in vivo* results, we observed reduced levels of Stat3 phosphorylation in response to leptin in SELENOM shRNA-expressing cells relative to controls expressing nontarget control (NTC) shRNA (Fig. 2B, C). We also utilized CRISPR/CAS9 technology to generate an edited mHypoE44 cell line where SELENOM expression was ablated (Fig. 2D). This cell line displayed reduced sensitivity to leptin stimulation (Fig. 2E, F), providing additional support that SELENOM impacts leptin signaling. To further confirm the role of SELENOM in leptin signaling, we also overexpressed SELENOM in mHypoE-44 cells (Fig. 3A). As anticipated, leptin treatment elicited significantly higher levels of Stat3 phosphorylation in SELENOM-overexpressing cells relative to controls (Fig. 3B, C). Taken together, these results demonstrate that SELENOM is a positive regulator of leptin signaling.

Prior *in vitro* studies demonstrated that SELENOM plays an important role in  $\text{Ca}^{2+}$  homeostasis (34). We next utilized live cell imaging to monitor changes in cytosolic  $\text{Ca}^{2+}$  induced by leptin treatment in our mHypoE-44 cell line. These cells were previously reported to express AGRP (10, 26), an established marker for a population of orexigenic hypothalamic neurons. The influence of leptin on AGRP neurons is inhibitory, leading to hyperpolarization and a reduction in cytosolic  $\text{Ca}^{2+}$  levels (27, 40). We found that leptin treatment of mHypoE-44 cells elicited a reduction in cytosolic  $\text{Ca}^{2+}$ , consistent with the notion that they display certain features of AGRP neurons. The leptin-induced reduction of cytosolic  $\text{Ca}^{2+}$  was abrogated in SELENOM shRNA-expressing cells (Fig. 4A, B), confirming prior observations of SELENOM involvement in both  $\text{Ca}^{2+}$  homeostasis and leptin signaling. Similar results were observed in our *Selenom*<sup>-/-</sup> cell line, as leptin failed to reduce cytosolic  $\text{Ca}^{2+}$  levels (Fig. 4C, D).

To gain further insight into the genes and signaling pathways regulated by SELENOM, we conducted microarray analysis on mHypoE-44 cells and hypothalamic tissue samples from 10-week-old mice. Genes showing fold changes greater than 1.5 and *p*-values <0.01 were considered differentially expressed genes (DEGs). Our analyses revealed 167 and 1983 DEGs in hypothalamic tissue and mHypoE-44 cells, respectively (Fig. 5A; Supplementary Table S1). We speculate that the smaller number of DEGs observed in hypothalamic tissue was largely due to the heterogeneous variety of cell types present in this sample. Among the identified DEGs, 11 genes were significantly altered in both hypothalamic tissue and mHypoE44 cells (Fig. 5B). One gene of significant interest was the thioredoxin interacting protein (TXNIP), a known negative regulator of TXN and mTOR-dependent signaling (18, 28), which was found downregulated in both tissue and cells. Moreover, of particular relevance to our study, TXNIP has also been implicated in the modulation of hypothalamic leptin signaling (3, 4).

Given that SELENOM is considered a member of the TXN superfamily, we speculated that decreased TXNIP expression may be a compensatory response to SELENOM ablation. To examine the influence of SELENOM on the TXN system, we performed a comprehensive evaluation of the TXN system in the samples used for our microarray analysis. Western blot analysis of hypothalamic samples confirmed that TXNIP expression was significantly attenuated by SELENOM deficiency, whereas levels of TXN1, TXN2, TXNRD1, and TXNRD2 were comparable between genotypes (Fig. 6A, B). In hypothalamic samples, TXN activity (Fig. 6C) was significantly lower in *Selenom*<sup>-/-</sup> samples, whereas TXNRD activity (Fig. 6D) did not differ. Parallel analysis of mHypoE-

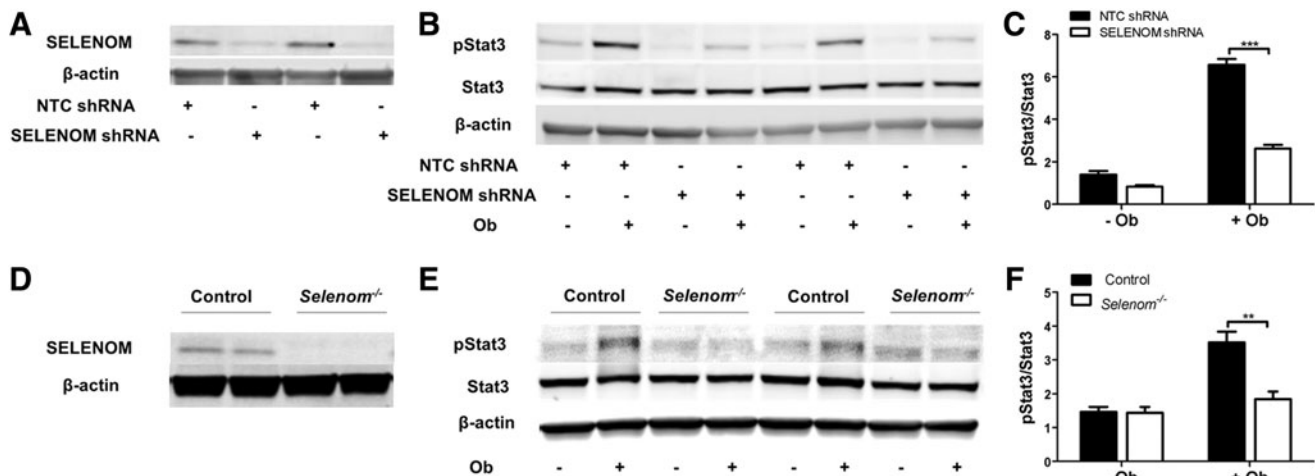


**FIG. 2. SELENOM deficiency impairs leptin signaling in mHypoE-44 cells.** (A) Verification of shRNA-mediated knockdown of SELENOM by Western blot. (B) Western blot analysis of leptin-induced STAT3 signaling in shRNA-treated mHypoE-44 cells. Cells were serum-starved for 4 h and then challenged with 100 nM leptin (Ob) for 45 min. (C) Two-way ANOVA analysis determined significant main effects for leptin ( $F_{(1,20)} = 144.2$ ,  $p < 0.001$ ), shRNA ( $F_{(1,20)} = 342.37$ ,  $p < 0.001$ ), and a significant interaction ( $F_{(1,20)} = 80.69$ ,  $p < 0.001$ ). Post-tests showed that leptin-induced Stat3 phosphorylation was diminished in SELENOM shRNA samples ( $t_{10} = 14.84$ ,  $p < 0.001$ ). (D) Verification of CRISPR/Cas9-mediated ablation of SELENOM by Western blot. (E) Western blot analysis of leptin-induced STAT3 signaling in control and *Selenom*<sup>-/-</sup> mHypoE-44 cells. (F) Two-way ANOVA analysis showed main effects for leptin ( $F_{(1,12)} = 14.77$ ,  $p = 0.0023$ ), genotype ( $F_{(1,12)} = 30.46$ ,  $p < 0.001$ ), and a significant interaction ( $F_{(1,12)} = 13.73$ ,  $p = 0.003$ ). Post-tests showed that leptin-induced Stat3 phosphorylation was diminished in *Selenom*<sup>-/-</sup> samples ( $t_6 = 5.337$ ,  $p < 0.01$ ). \*\* $p < 0.01$ , \*\*\* $p < 0.001$  compared with control group. NTC, nontarget control; shRNA, short hairpin RNA.

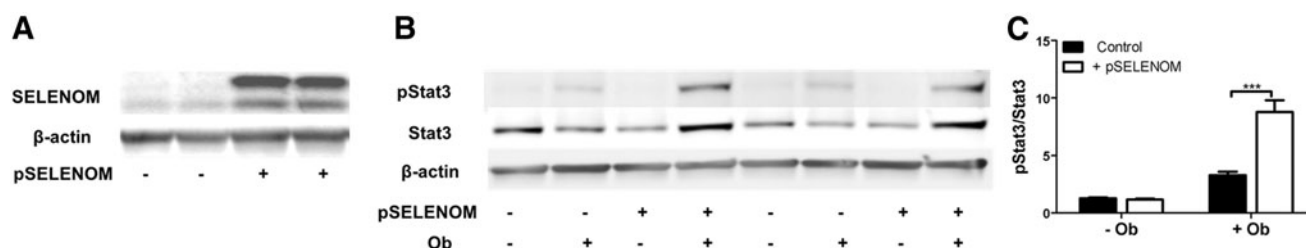


**FIG. 3. SELENOM overexpression promotes leptin signaling in mHypoE-44 cells.** (A) Verification of SELENOM overexpression by Western blot. (B) Western blot analysis of leptin-induced STAT3 signaling. (C) Two-way ANOVA analysis revealed main effects for leptin ( $F_{(1,20)} = 26.16$ ,  $p < 0.001$ ), pSELENOM ( $F_{(1,20)} = 83.98$ ,  $p < 0.01$ ), and a significant interaction ( $F_{(1,20)} = 28.84$ ,  $p < 0.001$ ). Post-tests showed that leptin-induced Stat3 phosphorylation was elevated in SELENOM-overexpressing (+pSELENOM) cells ( $t_{10} = 7.414$ ,  $p < 0.001$ ). \*\*\* $p < 0.001$  compared with control group.

44 samples provided verification of reduced TXNIP levels in SELENOM-deficient cells (Fig. 6E, F). Likewise, no differences between genotypes were observed in the protein levels of TXN1, TXN2, TXNRD1, and TXNRD2 in cell culture samples. Activity assays showed both reduced TXN and TXNRD activity in mHypoE-44 cells lacking SELENOM (Fig. 6G, H). The reason that SELENOM deficiency would impact TXNRD activity in cell culture and not hypothalamic tissue is not entirely clear, but it is likely related to the vast differences between an actual brain structure consisting of multiple cell types and a clonal, immortalized cell line.

We next performed an additional set of studies to assess whether SELENOM possesses intrinsic TXN and/or TXNRD activity. First, using anti-SELENOM conjugated agarose beads, we immunoprecipitated SELENOM from hypothalamic tissue samples (Fig. 7A). Levels of SELENOM were enriched in the eluate fraction, whereas SELENOM was undetected in the unbound flow-through sample. In contrast, SELENOM was present in the flow-through when beads were conjugated with control Immunoglobulin G (IgG). We then evaluated TXN activity in samples either enriched (eluate) or depleted (flow-through) of SELENOM (Fig. 7B). Eluates

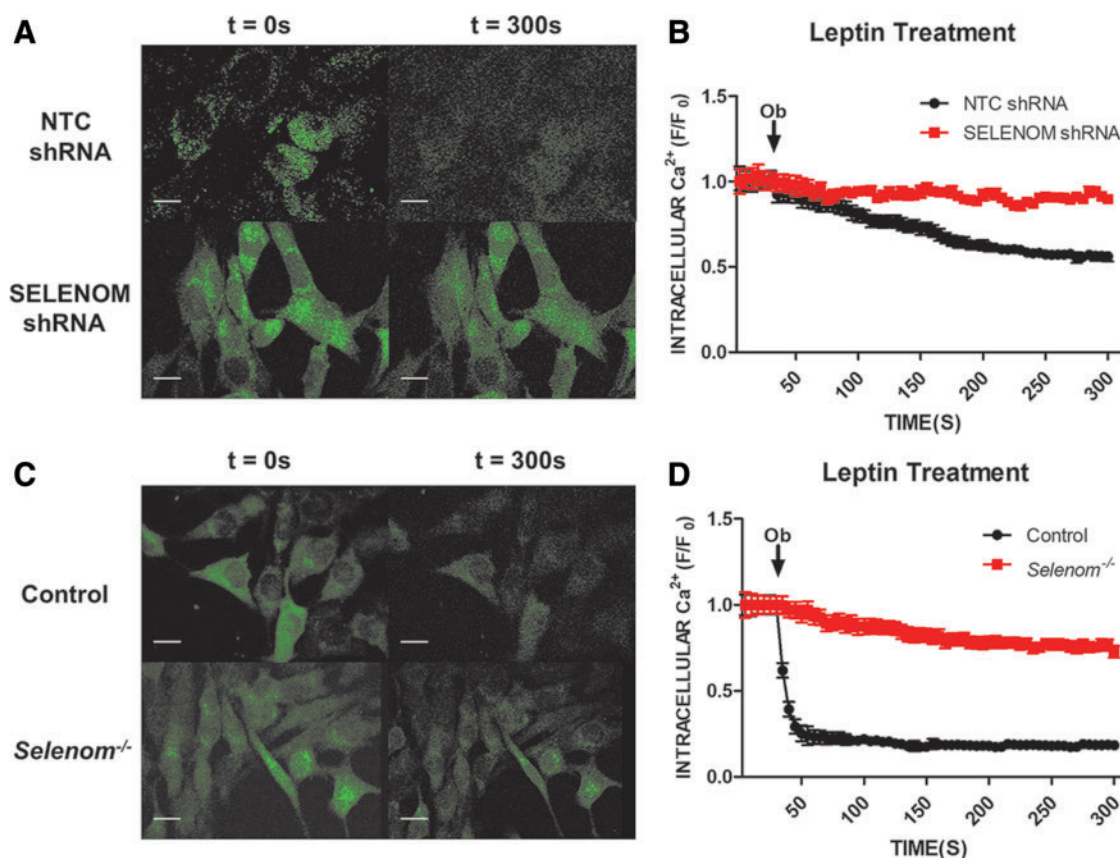
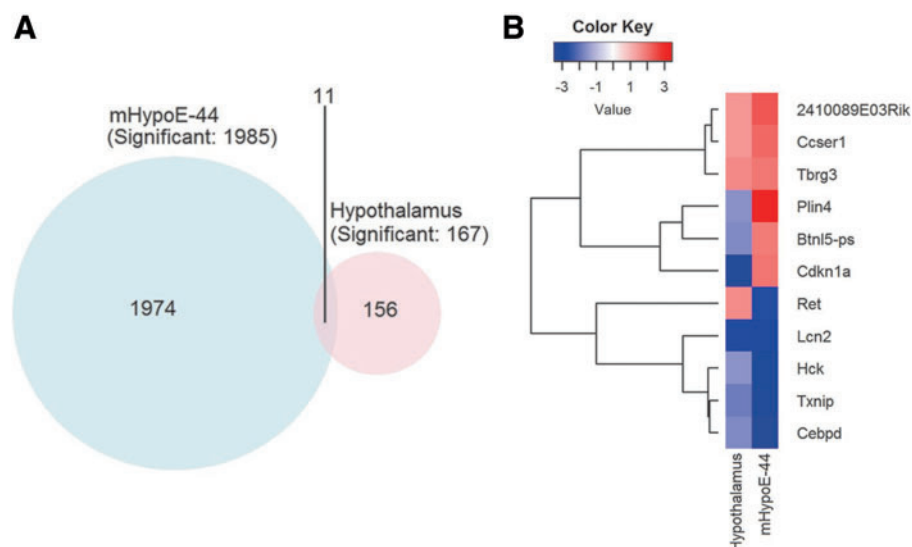


**FIG. 4. SELENOM deficiency impedes leptin-induced reduction of cytosolic Ca<sup>2+</sup> levels in mHypoE-44 cells.** (A, C) Confocal images showing cytosolic Ca<sup>2+</sup> levels before ( $t = 0$ s) and after treatment with leptin (Ob) ( $t = 300$ s). (B, D) Both shRNA-mediated knockdown (B) and CRISPR/CAS9-mediated knockout (D) of SELENOM impeded the leptin-induced reduction of cytosolic Ca<sup>2+</sup> observed in control samples. Scale bar = 20  $\mu$ m. Color images are available online.

**FIG. 5. Microarray analysis of SELENOM deficiency in hypothalamic tissue and mHypoE-44 cells.** (A) Venn diagram (top) showing the number of DEGs determined by the microarray analysis on mHypoE-44 cells and hypothalamic tissue. (B) Eleven DEGs were affected in both hypothalamic tissue and mHypoE44 cells. Heatmap plot (bottom) of these 11 DEGs, with upregulation and downregulation represented by red and blue, respectively. DEGs, differentially expressed genes. Color images are available online.



from WT mice displayed significantly higher levels of TXN activity in comparison to both WT samples immunoprecipitated with control IgG (Fig. 7B) and *Selenom*<sup>-/-</sup> samples immunoprecipitated with anti-SELENOM (Fig. 7C). TXN activity was comparable in the flow-through fractions from all groups analyzed. Similar experiments were conducted to evaluate TXNRD activity in SELENOM-enriched samples (Fig. 7D, E). Levels of TXNRD activity were similar in all eluate fractions analyzed and were several fold lower than those observed in flow-through fractions. In summary, these experiments show that SELENOM contributes to the hypothalamic TXN system by means of intrinsic TXN activity.

To further validate the functional contribution of SELENOM to TXN activity, we also assessed nuclear factor kappa-light-enhancer of activated B-cells (NF- $\kappa$ B) activation in our mHypoE-44 cell line. TXN has been previously shown to promote NF- $\kappa$ B DNA binding by means of disulfide bond reduction and denitrosylation on the p50 and p65 subunits, respectively (19, 25). Moreover, leptin is also known to stimulate NF- $\kappa$ B activation (6, 17). Thus, we examined NF- $\kappa$ B DNA binding under baseline conditions (-Ob) and in response to treatment with either leptin or 10% fetal bovine serum (FBS). As anticipated, both leptin and FBS promoted NF- $\kappa$ B activation (Fig. 8A), as two-way analysis of variance (ANOVA) analysis showed a significant main effect for treatment. We also observed a significant main effect for genotype, with *Selenom*<sup>-/-</sup> cells exhibiting lower levels of NF- $\kappa$ B activation across all treatment conditions. Of additional significance, two important NF- $\kappa$ B target genes, CCAAT/enhancer-binding protein delta (CEBPD) and lipocalin 2 (LCN2), were found to be significantly downregulated by SELENOM deficiency in our microarray analysis. These changes in expression were validated by quantitative polymerase chain reaction (PCR) in our mHypoE-44 cell line, providing additional corroboration that SELENOM facilitates activation of the NF- $\kappa$ B pathway (Fig. 8B).

Our final set of experiments utilized flow cytometry to assess the influence of SELENOM on mitochondrial ROS (mtROS) and cell viability in the presence of ER stress. ER stress was induced by treating mHypoE-44 cells with the

SERCA pump inhibitor, thapsigargin (Tg) (4  $\mu$ M), for ~2 h before analysis. For this study, we utilized the fluorescent indicators, MitoSOX and SYTOX AADvanced (SYTOX AAD), to measure mtROS and cell death, respectively. This allowed for simultaneous detection of mtROS and cell viability in individual cells using separate fluorescent channels (Fig. 9A). We found that baseline mtROS levels were comparable between control and *Selenom*<sup>-/-</sup> cells and that Tg treatment led to a significant elevation in mtROS production (Fig. 9B, C). In response to Tg, *Selenom*<sup>-/-</sup> cells showed a trend toward increased mtROS that approached statistical significance relative to controls ( $p=0.056$ ). More apparent was the observation that *Selenom*<sup>-/-</sup> cells were especially vulnerable to the deleterious effects of ER stress, as indicated by increased levels of SYTOX AAD, a cell-impermeable nucleic acid stain for the detection of dead cells (Fig. 9D). On setting a threshold of SYTOX AAD fluorescence for dead cells using Fluorescence Minus One gating analysis, a significantly greater percentage of *Selenom*<sup>-/-</sup> cells were non-viable relative to corresponding control cells. This difference was observed in the untreated condition and further enhanced by ER stress (Fig. 9E). Overall, these cumulative results demonstrate that when confronted with ER stress, the presence of SELENOM allows cells to tolerate higher levels of mtROS and remain viable.

## Discussion

The importance of hypothalamic selenoproteins to leptin signaling was recently illuminated in a study involving conditional deletion of the Sec-specific tRNA (*Trsp*) in cells expressing Cre-recombinase under the control of the rat insulin promoter (*RIP-Cre*) (43). The resulting mouse model (*Trsp*<sup>RIP-Cre</sup>) had disrupted selenoprotein synthesis in both hypothalamus and pancreas, as RIP is usually expressed in pancreatic  $\beta$ -cells and within certain hypothalamic cells. On challenge with a high-fat diet (HFD), *Trsp*<sup>RIP-Cre</sup> mice displayed increased hypothalamic levels of oxidative stress and diminished leptin sensitivity relative to controls. Comparable results were not observed in another mouse model (*Trsp*<sup>Ins1-Cre</sup>) where Cre-recombinase expression was restricted to

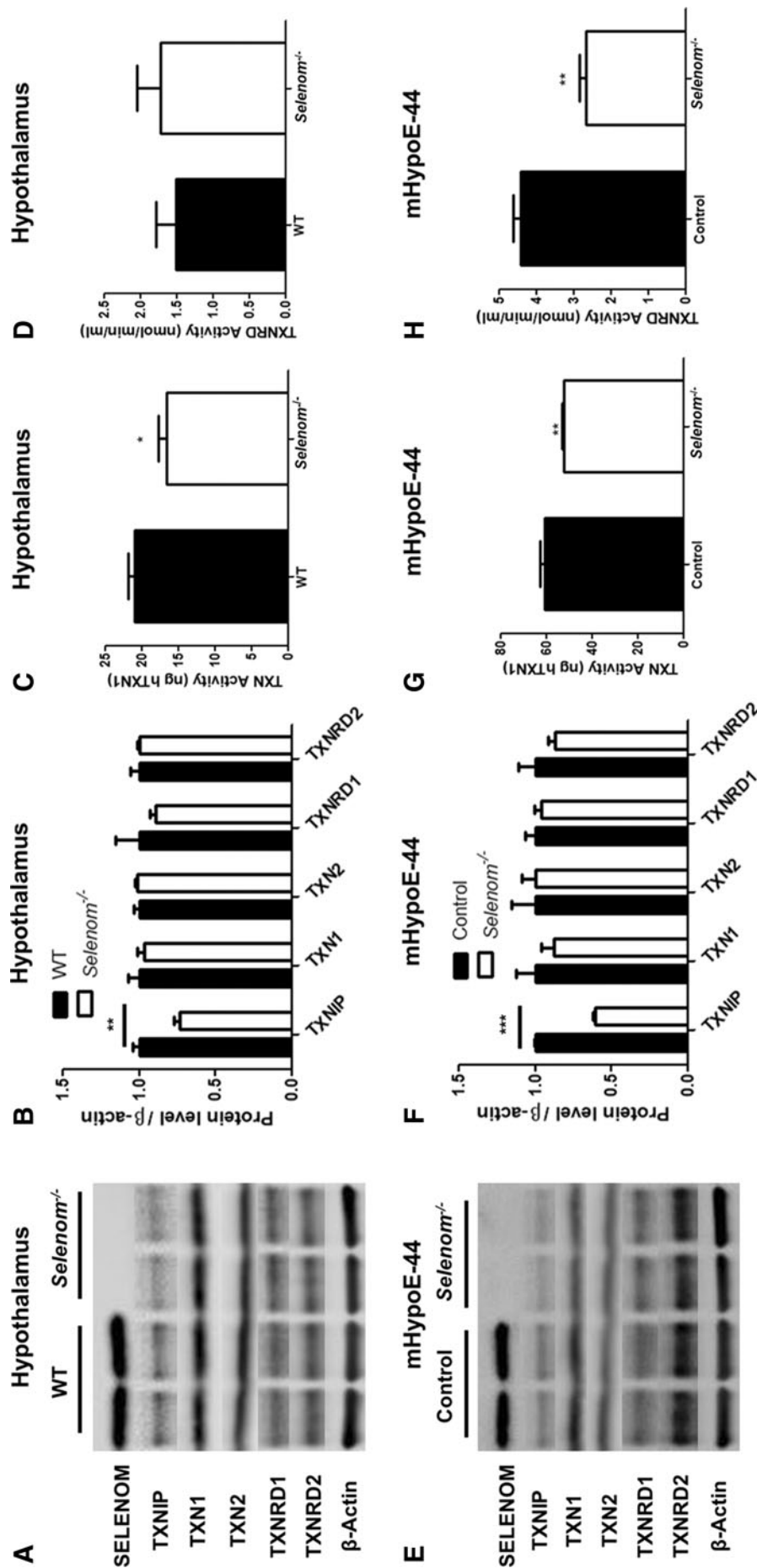
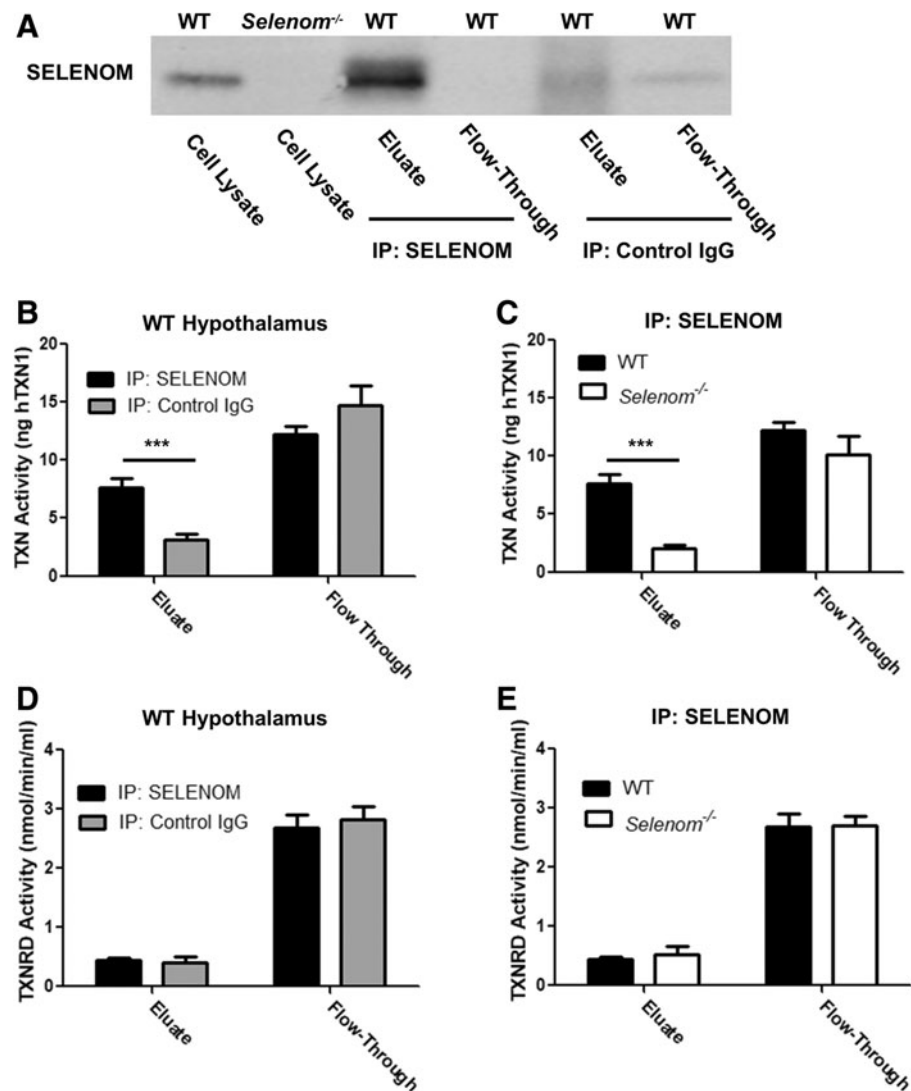


**FIG. 6. SELENOM deficiency significantly impacts TXN activity in hypothalamic tissue and mHypoE-44 cells.** (A, E) Western blot analysis of the TXN system in hypothalamic tissue (A) and mHypoE-44 cells (E). (B, F) TXNIP protein levels were significantly lower in both tissue ( $t_4 = 4.883$ ,  $p = 0.0081$ ) (B) and cells ( $t_4 = 19.61$ ,  $p < 0.001$ ) (F) devoid of SELENOM. (C, G) Levels of TXN activity were reduced by SELENOM deficiency in tissue ( $t_6 = 3.091$ ,  $p = 0.0214$ ) (C) and cells ( $t_{10} = 3.606$ ,  $p = 0.0048$ ) (G). (D, H) Levels of TXNRD activity were unaffected by SELENOM deficiency in tissue (D), but were significantly diminished in cells ( $t_8 = 6.527$ ,  $p = 0.0002$ ) (H). \* $p < 0.05$ , \*\* $p < 0.01$ , and \*\*\* $p < 0.001$  compared with control group. TXN, thioredoxin; TXNIP, thioredoxin interacting protein; TXNRD, thioredoxin reductase.



**FIG. 7. SELENOM has intrinsic TXN activity.** (A) Western blot analysis of hypothalamic tissue samples immunoprecipitated with antibodies against SELENOM and control IgG (negative control). Immunoprecipitation with the SELENOM antibody resulted in enriched levels of SELENOM in the eluate fraction and SELENOM depletion in the flow-through fraction. (B) SELENOM-immunoprecipitated WT samples displayed higher levels of TXN activity relative to WT samples immunoprecipitated with control IgG ( $t_6 = 4.537$ ,  $p = 0.0039$ ). (C) SELENOM-immunoprecipitated WT samples exhibited higher levels of TXN activity than those derived from *Selenom*<sup>-/-</sup> mice ( $t_6 = 6.328$ ,  $p = 0.0007$ ). (D) Levels of TXNRD activity were comparable in WT samples immunoprecipitated with antibodies against SELENOM and control IgG. (E) TXNRD activity levels were similar in SELENOM-immunoprecipitated samples from WT and *Selenom*<sup>-/-</sup> mice. \*\*\* $p < 0.001$  compared with control group. IgG, Immunoglobulin G.



pancreatic  $\beta$ -cells by an alternative promoter (*Ins1-Cre*), leading the authors to conclude that selenoprotein synthesis within the hypothalamus, but not the pancreas, is necessary for normal leptin sensitivity (43). Our results build on these findings and specifically delineate SELENOM as an important mediator of hypothalamic leptin signaling.

The data presented herein add to an accumulating body of evidence indicating that cellular redox status is a critical influence on leptin sensitivity. SELENOM is a member of the TXN superfamily, a group of oxidoreductases that catalyze disulfide bond formation by means of a thiol-disulfide exchange. The two defining features of TXNs are: (i) a CxxC active site motif and (ii) a characteristic tertiary structure consisting of four antiparallel beta sheets sandwiched between three alpha helices referred to as a TXN fold (24). In the case of SELENOM, the second cysteine residue of the active site motif is replaced by Sec, a substitution believed to accelerate thiol-like/disulfide exchange reactions (16). Disulfide bonds in TXNs are reduced by TXNRDs through an NADPH-dependent mechanism where electrons are taken from NADPH by TXNRDs and transferred to TXNs. TXN, TXNRD, and NADPH together constitute the TXN system, an antioxidant system essential

to mammalian life (1). Disturbances in the TXN system have been linked to metabolic syndrome (38), most prominently through TXNIP (31). This protein binds TXN with high affinity and effectively silences its ability to reduce target substrates (28). In response to severe ER stress, TXNIP is rapidly upregulated through the IRE1 and PERK pathways, leading to activation of the NLRP3 inflammasome and subsequent cell death (21, 29). Hypothalamic TXNIP also appears to be a significant player in energy metabolism, as experimental studies found that hypothalamic-specific knockdown of TXNIP protects against an HFD (4). Further studies by the same research group also demonstrated that overexpression of TXNIP in AGRP neurons reduces energy expenditure and impairs leptin sensitivity (3). In our study, TXNIP levels were significantly attenuated by SELENOM deficiency, an outcome that we hypothesize was a countermeasure to boost TXN activity and mitigate redox imbalance. Nevertheless, the reduction in TXNIP expression was not sufficient to normalize TXN activity, as reduced TXN activity was observed in *Selenom*<sup>-/-</sup> samples.

To our surprise, SELENOM deficiency did not alter the expression of PTP1B or SOCS3, two established

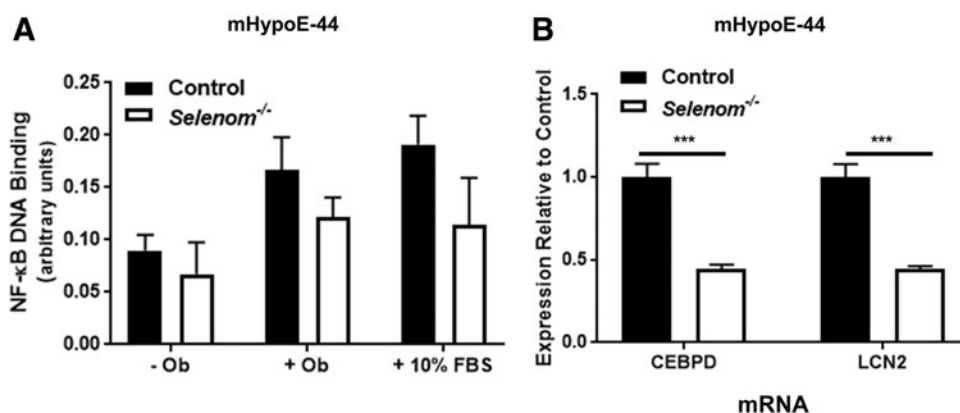


**FIG. 8. SELENOM promotes NF- $\kappa$ B activation in mHypoE-44 cells.** (A) NF- $\kappa$ B DNA binding activity was significantly impacted by both genotype ( $F_{(1,18)}=7.961$ ,  $p=0.0113$ ) and treatment ( $F_{(2,18)}=7.453$ ,  $p=0.0044$ ). *Selenom*<sup>-/-</sup> cells showed lower levels of NF- $\kappa$ B activation across all treatment conditions. (B) Levels of CEBPD ( $t_{10}=6.574$ ,  $p<0.001$ ) and LCN2 mRNA ( $t_{10}=6.837$ ,  $p<0.001$ ) were significantly reduced in *Selenom*<sup>-/-</sup> cells. \*\*\* $p<0.001$  compared with control group. CEBPD, CCAAT/enhancer-binding protein delta; LCN2, lipocalin 2; NF- $\kappa$ B, nuclear factor kappa-light-enhancer of activated B-cells.

suppressors of intracellular leptin signaling known to be upregulated by ER stress (2, 33, 41, 44). In both our microarray studies on hypothalamic tissue and mHypoE-44 cells, neither of these genes was significantly affected, even when we decreased the stringency of the  $p$ -value to 0.05 for additional analysis. However, of the four genes found significantly downregulated in cells and tissue, three (CEBPD,

LCN2, TXNIP) represent documented NF- $\kappa$ B target genes (7, 22, 35). These array results are consistent with our finding that SELENOM promotes both TXN and NF- $\kappa$ B activity, as TXN is known to facilitate NF- $\kappa$ B signaling by reducing redox-sensitive cysteine residues in the p50/p65 heterodimer through disulfide bond reduction and denitrosylation (19, 25). Extensive crosstalk occurs between the

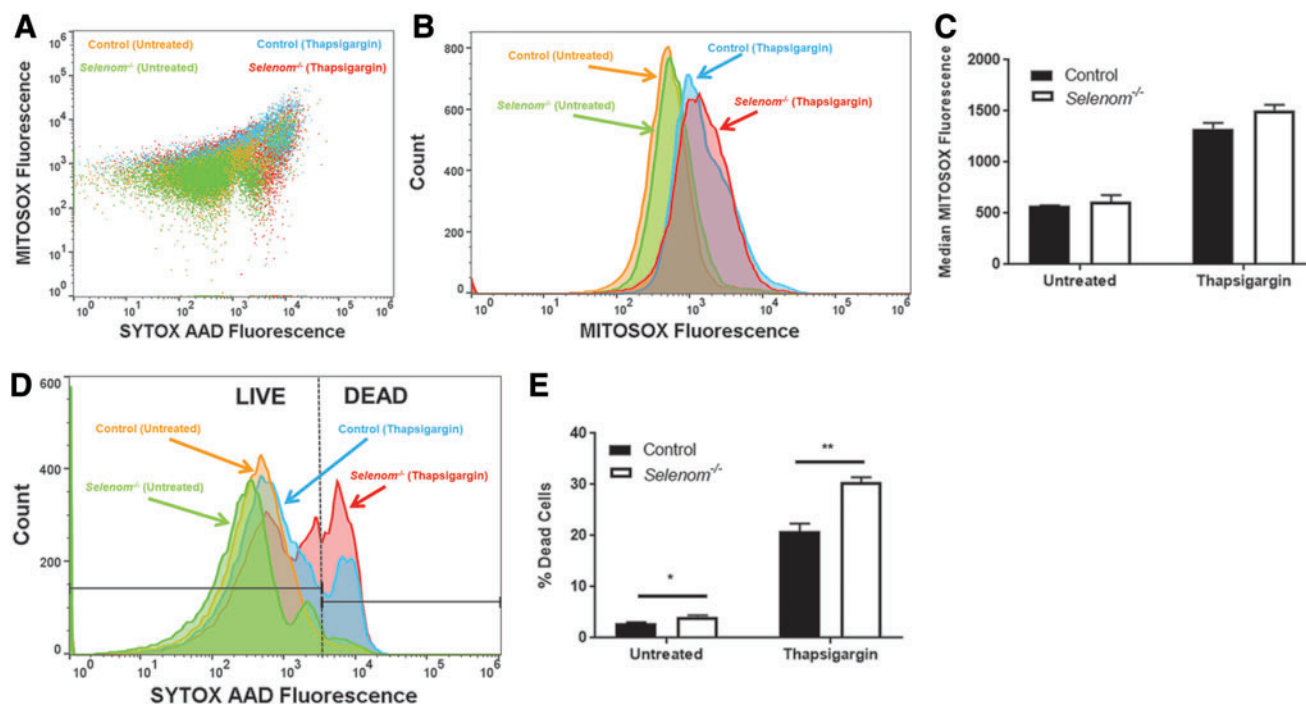


**FIG. 9. SELENOM protects against Tg-mediated ER stress in mHypoE-44 cells.** (A) Representative flow cytometry dot plots measuring mtROS (MITOSOX) and cell death (SYTOX AAD). (B) Representative histogram for MITOSOX fluorescence. (C) Two-way ANOVA analysis revealed a significant main effect of Tg treatment ( $F_{(1,12)}=255.3$ ,  $p<0.0001$ ) on mtROS levels, whereas the overall influence of genotype approached statistical significance ( $F_{(1,12)}=4.54$ ,  $p=0.0545$ ). (D) Representative histogram for SYTOX AAD fluorescence. (E) Cell death was significantly affected by both Tg treatment ( $F_{(1,12)}=89.88$ ,  $p<0.0001$ ) and genotype ( $F_{(1,12)}=5383$ ,  $p<0.0001$ ). The genotype  $\times$  treatment interaction was also significant ( $F_{(1,12)}=3.037$ ,  $p=0.0006$ ). Post-tests determined that *Selenom*<sup>-/-</sup> cells had a significantly higher proportion of cell death relative to controls both in the untreated condition ( $t_6=4.143$ ,  $p=0.012$ ) and in response to Tg ( $t_6=5.49$ ,  $p=0.003$ ). \* $p<0.05$ , \*\* $p<0.01$  compared with control group. ER, endoplasmic reticulum; mtROS, mitochondrial ROS; SYTOX AAD, SYTOX AAdvanced; Tg, thapsigargin. Color images are available online.



NF- $\kappa$ B and ER stress pathways, and both these pathways converge to stimulate transcriptional programs that promote antioxidant defense, cell survival, and inflammation (12, 42). There is also broad dialogue between the NF- $\kappa$ B and STAT3 pathways, which can be either antagonistic or cooperative in nature depending on the cell type and physiological context (14). For example, forced activation of the NF- $\kappa$ B pathway in the hypothalamus has been shown to occlude leptin-induced STAT3 signaling (45). Conversely, both the NF- $\kappa$ B and STAT3 pathways are constitutively active in many cancers and serve to promote cell survival and proliferation (5, 8, 13).

It is plausible that the decreased leptin sensitivity observed in *Selenom*<sup>-/-</sup> samples may result from disrupted communication between the leptin receptor and ER proteins involved in Ca<sup>2+</sup> signaling. This notion is supported by our Ca<sup>2+</sup> imaging data, in which SELENOM-deficient cells showed no discernible response to leptin. Of potential importance, two other ER-resident selenoproteins, SELENOK and SELENON, have been recently found to indirectly regulate Ca<sup>2+</sup> signaling *via* interactions with the inositol triphosphate receptor (11) and the SERCA2 pump (23), respectively. Although the precise mechanism remains to be established, it is conceivable that SELENOM acts by means of a similar redox mechanism involving the reduction of thiol groups on specific ER Ca<sup>2+</sup> channels and/or pumps.

In conclusion, our findings provide novel evidence revealing that SELENOM is a positive modulator of both leptin signaling and TXN activity in the hypothalamus (Fig. 10). *Selenom*<sup>-/-</sup> mice were observed to develop obesity and leptin resistance in earlier studies, but whether impairments in leptin signaling were the cause or a consequence of obesity was undetermined (32). The results of this study conclusively show that SELENOM deficiency impairs leptin signaling both *in vitro*, in immortalized hypothalamic cells, and *in vivo*, in 10-week-old nonobese mice. Moreover, our data demonstrate that SELENOM exhibits intrinsic TXN activity and represents an important contributor to the overall TXN antioxidant system in the hypothalamus.

## Materials and Methods

### Mice

Male wild-type and *Selenom*<sup>-/-</sup> mice on a C57BL/6N background were born and bred in the University of Hawaii Vivarium as previously described (32). All animals were group-housed and fed standard lab chow containing ~0.25 ppm Se. All procedures and experimental protocols were approved by the University of Hawaii's Institutional Animal Care and Use Committee.

### In vivo leptin challenge

Ten-week-old mice were fasted overnight, given an intraperitoneal injection of leptin (1  $\mu$ g leptin/g body weight), and sacrificed 1 h later by CO<sub>2</sub> asphyxiation. Whole brains were quickly removed, and the hypothalamus was isolated under a dissecting microscope and snap-frozen for later analyses.

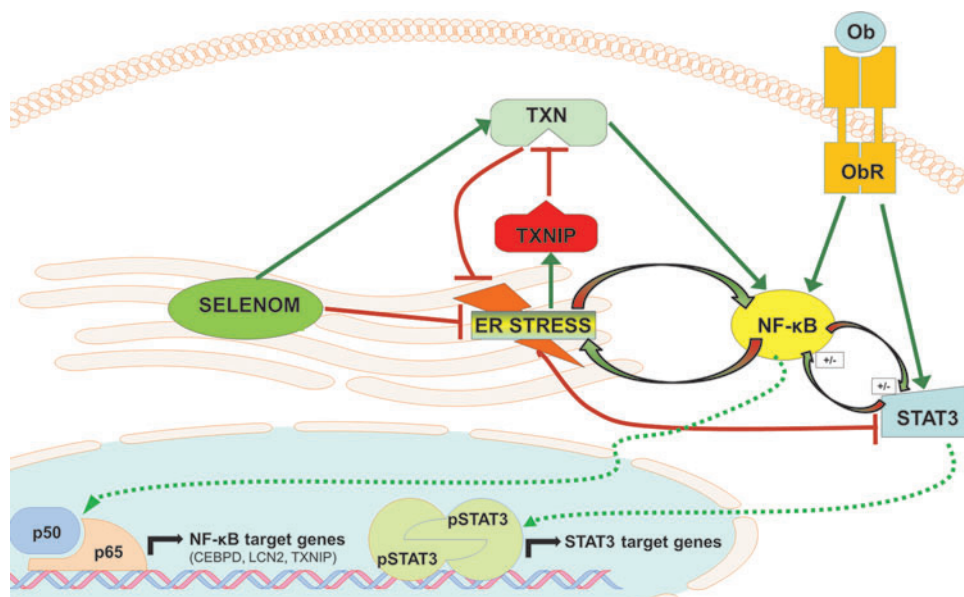
### Hypothalamic dissection

Mouse brains were briefly immersed in 0.32 M ice-cold sucrose and then placed ventral side up in a mouse brain matrix with slice intervals of 1 mm. A 3-mm-thick coronal section containing the hypothalamus was obtained by placing one razor blade at the level of the optic chiasm and a second blade 3 mm posterior to the first. The resulting section was placed on filter paper, and the hypothalamus was extracted with a scalpel under a dissecting microscope. Cuts were made at the roof of the third ventricle dorsally and at the fornix laterally to dissociate the hypothalamus from surrounding tissue.

### Antibodies and chemicals

The primary antibodies used in these experiments were rabbit anti-phospho-Stat3 Tyr705 (Cat # 9145, 1:1000; Cell Signaling Technology, Danvers, MA), rabbit anti-Stat3 (Cat # 8768, 1:1000; Cell Signaling), mouse anti-SELENOM (Cat # sc-514952, 1:500; Santa Cruz Biotechnology, Dallas, TEX), mouse anti-TXN (Cat # sc-166393, 1:500; Santa

**FIG. 10. Hypothalamic SELENOM promotes ER homeostasis and TXN activity.** SELENOM enhances activity of the TXN system, which serves to attenuate ER stress and facilitate activation of the NF- $\kappa$ B pathway. Leptin also promotes NF- $\kappa$ B activation in parallel with its documented effect on STAT3 signaling. On stimulation, both NF- $\kappa$ B and STAT3 translocate to the nucleus and act as transcription factors on a host of target genes. CEBPD, LCN2, and TXNIP comprise NF- $\kappa$ B target genes that are significantly downregulated by SELENOM deficiency. Color images are available online only.



Cruz), mouse anti-TXN 2 (Cat # sc-13320, 1:500; Santa Cruz), rabbit anti-TXNRDs 1 (Cat # NBP1-96738, 1:1000; Novus Biologicals, Littleton, CO), mouse anti-TXNRDs 2 (Cat # 365714, 1:500; Santa Cruz), mouse anti-TXNIP (Cat # sc-13320, 1:500; Santa Cruz), and mouse anti- $\beta$ -Actin (Cat # 3700, 1:5000; Cell Signaling). Species-specific secondary antibodies were purchased from LI-COR Biosciences (Lincoln, NE). Recombinant mouse leptin (Ob) was purchased from R&D Systems (Cat # 498-OB, Minneapolis, MN) and diluted to a stock concentration of 1 mg/mL in 20 mM Tris-HCl, pH 8.0. For all *in vitro* studies, cells were serum-starved for 4 h and then treated with 100 nM Ob for 45 min before harvesting.

#### Western blotting

Samples were lysed by sonication in CelLytic MT buffer (Cat # C3228; Sigma-Aldrich, St. Louis, MO) containing protease/phosphatase inhibitors (Cat # 5872; Cell Signaling) and centrifuged at 14,000g to remove insoluble material. Forty micrograms protein samples were resolved on a denaturing 4–20% sodium dodecyl sulfate-polyacrylamide gel electrophoresis (SDS-PAGE) gel (Cat # 345003; Bio-Rad, Hercules, CA) and transferred to polyvinylidene fluoride membranes by electroblotting. The membranes were then blocked in Odyssey blocking buffer in PBS (LI-COR) for 30 min and incubated with specific primary antibodies at 4°C overnight. Blots were incubated with secondary antibodies (LI-COR) at room temperature for 30 min in the dark the next day. Signals were detected and analyzed by Image Studio Version 4.0 (LI-COR Odyssey).

#### Quantitative PCR

RNA was isolated by using the RNeasy micro kit (Cat # 74004; Qiagen, Hilden, Germany). cDNA was synthesized by using a High-Capacity cDNA Reverse Transcription Kit (Cat # 4368814; Thermo Fisher). Amplification of cDNA (10 ng) was conducted in duplicate by using SYBR green kits (Cat # 4309155; Thermo Fisher) on a 480 real-time PCR machine (Roche Applied Science, Penzberg, Germany). Results were calculated by using the  $\Delta\Delta^{-CT}$  method and normalized to the hypoxanthine guanine phosphoribosyl-transferase (HPRT) housekeeping gene. The sequences of the forward and reverse primers used in our quantitative polymerase chain reaction studies were as follows: CEBPD (Forward 5'-TCAGCGCTACATTGACTCC-3'; Reverse 5'-TTGTGGTTGCTGTTGAAGAGG-3'), HPRT (Forward 5'-TCCTCCTCAGACCGCTTTT-3'; Reverse 5'-CCTGGTTCATCATCGCTAATC-3'), LCN2 (Forward 5'-CAATAGCTACAATGTCACCTCC-3'; Reverse 5'-AGGATACCTGTGCATATTTCCC-3'), and SELENOM (Forward 5'-GACATCAACTGTACCACAACC-3'; Reverse 5'-CTGGTAATTTGGCTTAACAGC-3').

#### Cell culture

The hypothalamic cell line, mHypoE-44, was purchased from Cellutions (Cat # CLU136, Toronto, OR) and grown in Dulbecco's modified Eagle medium (Cat # D5671; Sigma) containing 10% FBS (Cat # 16140089; Thermo Fisher) and 1% penicillin/streptomycin (Cat # 10378016; Thermo Fisher) in a humidified incubator with 5% CO<sub>2</sub> at 37°C. These are immortalized hypothalamic neurons derived from mouse embryonic hypothalamic primary cultures by retroviral

transfer of SV40 T-Ag. Although mHypoE-44 cells express the leptin receptor (ObR), we found that leptin responses were weak unless cells were transfected with an exogenous plasmid expressing the ObR. Therefore, for all leptin stimulation studies, cells were transfected with an ObR-expressing construct (gift from Christian Bjorbaek's Lab). For overexpression studies, we utilized a SELENOM overexpression vector (pSELENOM) that was created by subcloning SELENOM cDNA into the pSelExpress1 vector (gift from Vadim Gladyshev's Lab). In all studies involving leptin stimulation, cells at 70% confluency were transfected 2 days before imaging/treatment by using Lipofectamine 2000.

#### Generation of stably transfected mHypoE-44 cell lines

Constructs of shRNA for mouse SELENOM and an NTC were subcloned into the pTRIPZ vectors with the Tet-On inducible system with red fluorescent protein (Thermo Fisher Scientific). Hypothalamic cells at 70–80% confluency were transfected with pTRIPZ vectors containing either SELENOM or NTC shRNA by using Lipofectamine 2000. Stably transfected cells were selected by incubating in media containing puromycin (Cat # P8833, 1.5  $\mu$ g/mL; Sigma) for 7 days. For experiments using stably transfected cells, doxycycline (Cat # D9891, 2  $\mu$ g/mL; Sigma) was added to the media 48 h before experimentation to induce TurboRFP/shRNAmir expression.

#### CRISPR/Cas9-mediated editing of Selenom in mHypoE-44 cells

Cells were first transfected with a pSpCase9(BB)-2A-green fluorescent protein (GFP) (Addgene, Cambridge, MA) plasmid. After 24 h, GFP-positive cells were sorted by using an FACSaria flow cytometer (BD Bioscience, San Jose, CA). GFP-expressing cells were allowed to recover for an additional 24 h period and were then transfected with Integrated DNA Technologies (Coralville, IA) universal tracrRNA and guide crRNA targeting exon 1 of the *Selenom* gene. After another 24-h recovery period, cells were subjected to a second round of sorting for GFP-positive cells and seeded in 96-well plates at a density of 1 cell/well. These clones were grown into colonies and screened by PCR and Western blot to verify absence of SELENOM.

#### Calcium imaging

Cytosolic Ca<sup>2+</sup> levels were measured by using the Ca<sup>2+</sup> fluorescent dye Fluo-4 (Cat # F14201; Thermo Fisher). Cells were loaded with 5  $\mu$ M Fluo-4 and incubated for 30 min at 37°C immediately before imaging. They were then washed three times with Live Cell Imaging Solution (Cat # A14291DJ; Thermo Fisher), and coverslips were mounted onto RC-25F chambers (Cat # 64-0233; Warner Instruments, Hamden, CT) and placed in the mount of an inverted Nikon PCM 2000 confocal microscope located in the Kakaako Health Sciences Microscopy and Imaging Core Facility. Cells were excited by a 488-nm laser, and images were captured by using a 40 $\times$  oil objective and a 515–565-nm emission filter. Responses were recorded as a time course, consisting of confocal images taken at 5 s intervals for a total of 300 s. Leptin (100 nM) was added at 30 s. Using ImageJ software, fluorescence was converted to signal intensity and normalized to baseline (F/F<sub>0</sub>) for quantification purposes.

Ionomycin (Cat # I9657, 1  $\mu\text{g}/\text{mL}$ ; Sigma) was used as a positive control to elicit maximal  $\text{Ca}^{2+}$  responses.

#### Microarray analysis

RNA samples were sent to the University of Hawaii Cancer Center Genomics Core Facility for microarray analysis. RNA integrity was first validated on an Agilent 2100 Bioanalyzer. One hundred nanograms of total RNA was then used for the GeneChip whole-transcript assay followed by hybridization to Clariom S Mouse Arrays (Cat # 902930; Affymetrix, Santa Clara, CA). Arrays were washed, stained, and scanned by using a GeneChip Fluidics Station 450 and a GeneChip Scanner (Affymetrix). CEL files generated from Clariom S Mouse Arrays were analyzed by Transcriptome Analysis Console software v4.0 (Affymetrix). Genes with fold-changes greater than 1.5 and  $p$ -values  $<0.01$  between *Selenom*<sup>-/-</sup> and control samples were considered differentially expressed.

#### Antioxidant activity assays

TXN (Cat # 11527; Cayman Chemical, Ann Arbor, MI) and TXNRD activity (Cat # 10007892; Cayman) were measured by using commercially available kits according to the manufacturer's instructions. For both of these assays, samples were run in duplicate and consisted of 20  $\mu\text{g}$  of total protein per well. TXN activity was determined by measuring the reduction of insulin disulfides in the presence of a relative excess of NADPH and TXNRD. For this assay, human recombinant TXN1 was used both as a positive control and to generate a standard calibration curve. One unit of TXN activity was defined as being equivalent to 1 ng human recombinant TXN1, as determined by the calibration curve (Supplementary Fig. S1). As a negative control for TXN activity, the potent TXN inhibitor, PX12 (Cat # 14192, 5  $\mu\text{M}$ ; Cayman Chemical), was also incorporated (Supplementary Fig. S2). TXNRD activity was determined by using a colorimetric assay based on the reduction of DTNB [5,5'-dithiobis(2-dinitrobenzoic acid); Ellman's reagent] to TNB (5-thio-2-nitrobenzoic acid), which yields a yellow product that is measured at 405 nm. For each sample, DNTB reduction is measured in the absence and presence of sodium aurothiomalate, a specific inhibitor of TXNRD. This allows for the correction of TXNRD-independent reduction of DNTB. A positive control of purified rat liver TXNRD was also included to verify the specificity of this assay (Supplementary Fig. S3).

#### SELENOM immunoprecipitation

SELENOM was immunoprecipitated from hypothalamic tissue by using a mouse monoclonal SELENOM antibody conjugated to agarose beads (Cat # sc-514952 AC, 500  $\mu\text{g}/\text{mL}$ ; Santa Cruz). As a negative control, mouse IgG-conjugated agarose beads were also utilized (Cat # sc-2343, 500  $\mu\text{g}/\text{mL}$ ; Santa Cruz). For immunoprecipitation, 500  $\mu\text{g}$  of total protein was incubated overnight at 4°C with 50  $\mu\text{L}$  of antibody-conjugated beads. The next morning, samples were spun and supernatants (flow-through) were captured. Beads were then washed and spun three times. After the wash steps, each sample was allocated into three separate tubes (15  $\mu\text{L}$  each) to assess protein levels (Western blot), TXN activity, and TXNRDs activity. For Western blotting, 15  $\mu\text{L}$  of beads were mixed with 15  $\mu\text{L}$  of loading dye and boiled at 95°C for

10 min. Samples were then spun, and supernatants were resolved on a denaturing 4–20% SDS-PAGE gel. For the activity assays (TXN, TXNRD), beads were directly added to the 96-well plate where the assay was conducted.

#### NF- $\kappa$ B DNA binding assay

NF- $\kappa$ B activation was determined by using a commercially available kit (Cat # 10007889; Cayman) that detects DNA binding of the p65 subunit of the NF- $\kappa$ B complex. For this assay, nuclear fractions were first isolated from mHypoE-44 cells by using a nuclear extraction kit (Cat # 10009277; Cayman). Nuclear protein samples were run in duplicate and consisted of 5  $\mu\text{g}$  of total protein per well. To verify assay specificity and monitor the dynamic range, serial dilutions of a positive control for NF- $\kappa$ B activation were run in parallel to generate a standard curve. One unit of NF- $\kappa$ B activity was defined as being equivalent to the response of the undiluted positive control. Also included to verify specificity was a negative control where NF- $\kappa$ B competitor dsDNA was co-administered in conjunction with the undiluted positive control (Supplementary Fig. S4).

#### Flow cytometry

For measurement of mtROS, samples containing  $4 \times 10^5$  cells (volume = 1 mL) were incubated at 37°C for 15 min with 1  $\mu\text{M}$  of MitoSOX Red Superoxide Indicator (Cat # 36008; Thermo Fisher). ER stress was induced in select samples at the time of MitoSOX incubation by co-administration of 4  $\mu\text{M}$  Tg (T9033; Sigma). Cells were then pelleted, washed, and resuspended in PBS supplemented with 25 mM 4-(2-hydroxyethyl)-1-piperazineethanesulfonic acid, 1 mM ethylenediaminetetracetic acid, and 1% FBS. Immediately before analysis with the flow cytometer, 1  $\mu\text{M}$  of SYTOX AAD (Cat # S10349; Thermo Fisher) was added to samples for identification of dead cells. Cells were analyzed by using an Attune NxT flow cytometer (Thermo Fisher) and FlowJo software v10 (FlowJo LLC, Ashland, OR) housed in the Molecular and Cellular Immunology Core Facility at the University of Hawaii. Forward and side scatter gating was used to exclude debris, and single-cell discrimination was done to restrict analysis to single cells. Compensation was applied to correct for spectral overlap between MitoSOX and SYTOX AAD. For each condition, analysis was conducted on four separate samples consisting of 20,000–30,000 single cells.

#### Statistical analysis

Data were analyzed and plotted by using GraphPad Prism software 7.0. Statistical tests varied according the experiment and are indicated in the text and/or figure legends. Results are represented as means  $\pm$  standard error of the mean. A statistically significant difference was considered present at  $p < 0.05$ , unless otherwise noted.

#### Acknowledgments

This work was supported by National Institutes of Health Grants G12 MD007601, U54 MD007584, U54 MD007601, P20 GM103466, P30 GM114737, and pilot funds from G12 MD007601 and P20 GM113134 to M.W.P. The authors also thank Marla Berry for providing mentoring and access to facilities and experimental materials.

## Author Disclosure Statement

No competing financial interests exist.

## Supplementary Material

Supplementary Figures S1  
Supplementary Figures S2  
Supplementary Figures S3  
Supplementary Figures S4  
Supplementary Table S1

## References

- Arner ES and Holmgren A. Physiological functions of thioredoxin and thioredoxin reductase. *Eur J Biochem* 267: 6102–6109, 2000.
- Bjorbaek C, El-Haschimi K, Frantz JD, and Flier JS. The role of SOCS-3 in leptin signaling and leptin resistance. *J Biol Chem* 274: 30059–30065, 1999.
- Blouet C, Liu SM, Jo YH, Chua S, and Schwartz GJ. TXNIP in AgRP neurons regulates adiposity, energy expenditure, and central leptin sensitivity. *J Neurosci* 32: 9870–9877, 2012.
- Blouet C and Schwartz GJ. Nutrient-sensing hypothalamic TXNIP links nutrient excess to energy imbalance in mice. *J Neurosci* 31: 6019–6027, 2011.
- Bollrath J and Greten FR. IKK/NF-kappaB and STAT3 pathways: central signalling hubs in inflammation-mediated tumour promotion and metastasis. *EMBO Rep* 10: 1314–1319, 2009.
- Bouloumie A, Marumo T, Lafontan M, and Busse R. Leptin induces oxidative stress in human endothelial cells. *FASEB J* 13: 1231–1238, 1999.
- Cowland JB, Sorensen OE, Sehested M, and Borregaard N. Neutrophil gelatinase-associated lipocalin is up-regulated in human epithelial cells by IL-1 beta, but not by TNF-alpha. *J Immunol* 171: 6630–6639, 2003.
- De Simone V, Franze E, Ronchetti G, Colantoni A, Fantini MC, Di Fusco D, Sica GS, Sileri P, MacDonald TT, Pallone F, Monteleone G, and Stolfi C. Th17-type cytokines, IL-6 and TNF-alpha synergistically activate STAT3 and NF-kB to promote colorectal cancer cell growth. *Oncogene* 34: 3493–3503, 2015.
- Ferguson AD, Labunsky VM, Fomenko DE, Arac D, Chelliah Y, Amezcua CA, Rizo J, Gladyshev VN, and Deisenhofer J. NMR structures of the selenoproteins Sep15 and SelM reveal redox activity of a new thioredoxin-like family. *J Biol Chem* 281: 3536–3543, 2006.
- Fick LJ, Fick GH, and Belsham DD. Rhythmic clock and neuropeptide gene expression in hypothalamic mHypoE-44 neurons. *Mol Cell Endocrinol* 323: 298–306, 2010.
- Fredericks GJ, Hoffmann FW, Rose AH, Osterheld HJ, Hess FM, Mercier F, and Hoffmann PR. Stable expression and function of the inositol 1,4,5-triphosphate receptor requires palmitoylation by a DHHC6/selenoprotein K complex. *Proc Natl Acad Sci U S A* 111: 16478–16483, 2014.
- Garg AD, Kaczmarek A, Krysko O, Vandenabeele P, Krysko DV, and Agostinis P. ER stress-induced inflammation: does it aid or impede disease progression? *Trends Mol Med* 18: 589–598, 2012.
- Greten FR, Weber CK, Greten TF, Schneider G, Wagner M, Adler G, and Schmid RM. Stat3 and NF-kappaB activation prevents apoptosis in pancreatic carcinogenesis. *Gastroenterology* 123: 2052–2063, 2002.
- Grivennikov SI and Karin M. Dangerous liaisons: STAT3 and NF-kappaB collaboration and crosstalk in cancer. *Cytokine Growth Factor Rev* 21: 11–19, 2010.
- Hetz C. The unfolded protein response: controlling cell fate decisions under ER stress and beyond. *Nat Rev Mol Cell Biol* 13: 89–102, 2012.
- Hondal RJ, Marino SM, and Gladyshev VN. Selenocysteine in thiol/disulfide-like exchange reactions. *Antioxid Redox Signal* 18: 1675–1689, 2013.
- Jang PG, Namkoong C, Kang GM, Hur MW, Kim SW, Kim GH, Kang Y, Jeon MJ, Kim EH, Lee MS, Karin M, Baik JH, Park JY, Lee KU, Kim YB, and Kim MS. NF-kappaB activation in hypothalamic pro-opiomelanocortin neurons is essential in illness- and leptin-induced anorexia. *J Biol Chem* 285: 9706–9715, 2010.
- Jin HO, Seo SK, Kim YS, Woo SH, Lee KH, Yi JY, Lee SJ, Choe TB, Lee JH, An S, Hong SI, and Park IC. TXNIP potentiates Redd1-induced mTOR suppression through stabilization of Redd1. *Oncogene* 30: 3792–3801, 2011.
- Kelleher ZT, Sha Y, Foster MW, Foster WM, Forrester MT, and Marshall HE. Thioredoxin-mediated denitrosylation regulates cytokine-induced nuclear factor kappaB (NF-kappaB) activation. *J Biol Chem* 289: 3066–3072, 2014.
- Lee K, Tirasophon W, Shen X, Michalak M, Prywes R, Okada T, Yoshida H, Mori K, and Kaufman RJ. IRE1-mediated unconventional mRNA splicing and S2P-mediated ATF6 cleavage merge to regulate XBP1 in signaling the unfolded protein response. *Genes Dev* 16: 452–466, 2002.
- Lerner AG, Upton JP, Praveen PV, Ghosh R, Nakagawa Y, Igarria A, Shen S, Nguyen V, Backes BJ, Heiman M, Heintz N, Greengard P, Hui S, Tang Q, Trusina A, Oakes SA, and Papa FR. IRE1alpha induces thioredoxin-interacting protein to activate the NLRP3 inflammasome and promote programmed cell death under irremediable ER stress. *Cell Metab* 16: 250–264, 2012.
- Liu YW, Chen CC, Wang JM, Chang WC, Huang YC, Chung SY, Chen BK, and Hung JJ. Role of transcriptional factors Sp1, c-Rel, and c-Jun in LPS-induced C/EBPdelta gene expression of mouse macrophages. *Cell Mol Life Sci* 64: 3282–3294, 2007.
- Marino M, Stoilova T, Giorgi C, Bachi A, Cattaneo A, Auricchio A, Pinton P, and Zito E. SEP1N1, an endoplasmic reticulum-localized selenoprotein linked to skeletal muscle pathology, counteracts hyperoxidation by means of redox-regulating SERCA2 pump activity. *Hum Mol Genet* 24: 1843–1855, 2015.
- Martin JL. Thioredoxin—a fold for all reasons. *Structure* 3: 245–250, 1995.
- Matthews JR, Wakasugi N, Virelizier JL, Yodoi J, and Hay RT. Thioredoxin regulates the DNA binding activity of NF-kappa B by reduction of a disulphide bond involving cysteine 62. *Nucleic Acids Res* 20: 3821–3830, 1992.
- Mayer CM and Belsham DD. Palmitate attenuates insulin signaling and induces endoplasmic reticulum stress and apoptosis in hypothalamic neurons: rescue of resistance and apoptosis through adenosine 5' monophosphate-activated protein kinase activation. *Endocrinology* 151: 576–585, 2010.
- Muroya S, Funahashi H, Yamanaka A, Kohno D, Uramura K, Nambu T, Shibahara M, Kuramochi M, Takigawa M, Yanagisawa M, Sakurai T, Shioda S, and Yada T. Orexins (hypocretins) directly interact with neuropeptide Y, POMC and glucose-responsive neurons to regulate Ca<sup>2+</sup> signaling in a reciprocal manner to leptin: orexigenic neuronal

- pathways in the mediobasal hypothalamus. *Eur J Neurosci* 19: 1524–1534, 2004.
28. Nishiyama A, Matsui M, Iwata S, Hirota K, Masutani H, Nakamura H, Takagi Y, Sono H, Gon Y, and Yodoi J. Identification of thioredoxin-binding protein-2/vitamin D(3) up-regulated protein 1 as a negative regulator of thioredoxin function and expression. *J Biol Chem* 274: 21645–21650, 1999.
  29. Osowski CM, Hara T, O'Sullivan-Murphy B, Kanekura K, Lu S, Hara M, Ishigaki S, Zhu LJ, Hayashi E, Hui ST, Greiner D, Kaufman RJ, Bortell R, and Urano F. Thioredoxin-interacting protein mediates ER stress-induced beta cell death through initiation of the inflammasome. *Cell Metab* 16: 265–273, 2012.
  30. Ozcan L, Ergin AS, Lu A, Chung J, Sarkar S, Nie D, Myers MG, Jr., and Ozcan U. Endoplasmic reticulum stress plays a central role in development of leptin resistance. *Cell Metab* 9: 35–51, 2009.
  31. Parikh H, Carlsson E, Chutkow WA, Johansson LE, Storgaard H, Poulsen P, Saxena R, Ladd C, Schulze PC, Mazzini MJ, Jensen CB, Krook A, Bjornholm M, Tornqvist H, Zierath JR, Ridderstrale M, Altshuler D, Lee RT, Vaag A, Groop LC, and Mootha VK. TXNIP regulates peripheral glucose metabolism in humans. *PLoS Med* 4: e158, 2007.
  32. Pitts MW, Reeves MA, Hashimoto AC, Ogawa A, Kremer P, Seale LA, and Berry MJ. Deletion of selenoprotein M leads to obesity without cognitive deficits. *J Biol Chem* 288: 26121–26134, 2013.
  33. Ramirez S and Claret M. Hypothalamic ER stress: a bridge between leptin resistance and obesity. *FEBS Lett* 589: 1678–1687, 2015.
  34. Reeves MA, Bellinger FP, and Berry MJ. The neuroprotective functions of selenoprotein M and its role in cytosolic calcium regulation. *Antioxid Redox Signal* 12: 809–818, 2010.
  35. Sharif O, Bolshakov VN, Raines S, Newham P, and Perkins ND. Transcriptional profiling of the LPS induced NF-kappaB response in macrophages. *BMC Immunol* 8: 1, 2007.
  36. Sriburi R, Bommiasamy H, Buldak GL, Robbins GR, Frank M, Jackowski S, and Brewer JW. Coordinate regulation of phospholipid biosynthesis and secretory pathway gene expression in XBP-1(S)-induced endoplasmic reticulum biogenesis. *J Biol Chem* 282: 7024–7034, 2007.
  37. Tabas I and Ron D. Integrating the mechanisms of apoptosis induced by endoplasmic reticulum stress. *Nat Cell Biol* 13: 184–190, 2011.
  38. Tinkov AA, Bjorklund G, Skalny AV, Holmgren A, Skalnaya MG, Chirumbolo S, and Aaseth J. The role of the thioredoxin/thioredoxin reductase system in the metabolic syndrome: towards a possible prognostic marker? *Cell Mol Life Sci* 75: 1567–1586, 2018.
  39. Tung YC, Ma M, Piper S, Coll A, O'Rahilly S, and Yeo GS. Novel leptin-regulated genes revealed by transcriptional profiling of the hypothalamic paraventricular nucleus. *J Neurosci* 28: 12419–12426, 2008.
  40. van den Top M, Lee K, Whyment AD, Blanks AM, and Spanswick D. Orexin-sensitive NPY/AgRP pacemaker neurons in the hypothalamic arcuate nucleus. *Nat Neurosci* 7: 493–494, 2004.
  41. Williams KW, Liu T, Kong X, Fukuda M, Deng Y, Berglund ED, Deng Z, Gao Y, Liu T, Sohn JW, Jia L, Fujikawa T, Kohno D, Scott MM, Lee S, Lee CE, Sun K, Chang Y, Scherer PE, and Elmquist JK. Xbp1s in Pomc neurons connects ER stress with energy balance and glucose homeostasis. *Cell Metab* 20: 471–482, 2014.
  42. Xu C, Bailly-Maitre B, and Reed JC. Endoplasmic reticulum stress: cell life and death decisions. *J Clin Invest* 115: 2656–2664, 2005.
  43. Yagishita Y, Urano A, Fukutomi T, Saito R, Saigusa D, Pi J, Fukamizu A, Sugiyama F, Takahashi S, and Yamamoto M. Nrf2 improves leptin and insulin resistance provoked by hypothalamic oxidative stress. *Cell Rep* 18: 2030–2044, 2017.
  44. Zabolotny JM, Bence-Hanulec KK, Stricker-Krongrad A, Haj F, Wang Y, Minokoshi Y, Kim YB, Elmquist JK, Tartaglia LA, Kahn BB, and Neel BG. PTP1B regulates leptin signal transduction in vivo. *Dev Cell* 2: 489–495, 2002.
  45. Zhang X, Zhang G, Zhang H, Karin M, Bai H, and Cai D. Hypothalamic IKKbeta/NF-kappaB and ER stress link overnutrition to energy imbalance and obesity. *Cell* 135: 61–73, 2008.

Address correspondence to:

Dr. Matthew W. Pitts

Department of Cell and Molecular Biology

John A. Burns School of Medicine

University of Hawaii

651 Ilalo Street

Honolulu, HI 96813

USA

E-mail: mwpitts@hawaii.edu

Date of first submission to ARS Central, June 7, 2018; date of final revised submission, January 14, 2019; date of acceptance, January 15, 2019.

#### Abbreviations Used

AGRP = agouti-related peptide  
 ANOVA = analysis of variance  
 CEBPD = CCAAT/enhancer-binding protein delta  
 DEG = differentially expressed gene  
 ER = endoplasmic reticulum  
 FBS = fetal bovine serum  
 GFP = green fluorescent protein  
 HFD = high-fat diet  
 HPRT = hypoxanthine guanine phosphoribosyltransferase  
 IgG = Immunoglobulin G  
 LCN2 = lipocalin 2  
 mtROS = mitochondrial ROS  
 NF-κB = nuclear factor kappa-light-enhancer of activated B-cells  
 NTC = nontarget control  
 PCR = polymerase chain reaction  
 SDS-PAGE = sodium dodecyl sulfate-polyacrylamide gel electrophoresis  
 Se = selenium  
 Sec = selenocysteine  
 SELENOM = selenoprotein M  
 shRNA = short hairpin RNA  
 SYTOX AAD = SYTOX AAdvanced  
 Tg = thapsigargin  
 TXN = thioredoxin  
 TXNIP = thioredoxin interacting protein  
 TXNRD = thioredoxin reductase  
 WT = wild type  
 XBP1s = X-box binding protein 1